PHOTONICS Research

Optical forces of focused femtosecond laser pulses on nonlinear optical Rayleigh particles

Liping Gong,[1] Bing Gu,[1,*] Guanghao Rui,[1] Yiping Cui,[1] Zhuqing Zhu,[2] and Qiwen Zhan[3]

[1]Advanced Photonics Center, Southeast University, Nanjing 210096, Jiangsu, China
[2]Key Laboratory of Optoelectronic Technology of Jiangsu Province, School of Physical Science and Technology, Nanjing Normal University, Nanjing 210023, Jiangsu, China
[3]Department of Electro-Optics and Photonics, University of Dayton, 300 College Park, Dayton, Ohio 45469-2951, USA
*Corresponding author: gubing@seu.edu.cn

Received 30 October 2017; revised 10 December 2017; accepted 11 December 2017; posted 15 December 2017 (Doc. ID 311249); published 26 January 2018

The principle of optical trapping is conventionally based on the interaction of optical fields with linear-induced polarizations. However, the optical force originating from the nonlinear polarization becomes significant when nonlinear optical nanoparticles are trapped by femtosecond laser pulses. Herein we develop the time-averaged optical forces on a nonlinear optical nanoparticle using high-repetition-rate femtosecond laser pulses, based on the linear and nonlinear polarization effects. We investigate the dependence of the optical forces on the magnitudes and signs of the refractive nonlinearities. It is found that the self-focusing effect enhances the trapping ability, whereas the self-defocusing effect leads to the splitting of the potential well at the focal plane and destabilizes the optical trap. Our results show good agreement with the reported experimental observations and provide theoretical support for capturing nonlinear optical particles.

OCIS codes: (190.3270) Kerr effect; (140.7010) Laser trapping; (350.4990) Particles; (190.7110) Ultrafast nonlinear optics.

https://doi.org/10.1364/PRJ.6.000138

1. INTRODUCTION

Optical trapping, also known as optical tweezers, is a useful technique for noncontact and noninvasive manipulation of small particles using a focused laser beam [1]. This technique has wide applications in physics, chemistry, biology, and other disciplines [2,3]. Up to now, the stable optical trapping of micro- and nanoparticles has been extensively demonstrated by the use of a continuous-wave (CW) Gaussian laser beam [1–3], cylindrical vector beam [4], evanescent field [5], plasmonic field [6], and spinning light fields [7], etc. Lots of efforts have been devoted to trapping a variety of small objects, such as dielectric particles [1], metallic Rayleigh nanoparticles [4], semiconductor quantum dots [8], and biological cells [9].

Recently, the optical trapping technique has been extended by substituting a CW laser with high-repetition-rate femtosecond laser pulses [10–12]. With the femtosecond laser pulses, several novel phenomena have been observed, including the trapping split behavior in the process of capturing gold nanoparticles by femtosecond near-infrared laser pulses [13], a controllable directional ejection of optically trapped nanoparticles [14], and the immobilization dynamics of a single polystyrene sphere [15]. It should be noted that the optical force originating from the nonlinear polarization becomes significant and cannot be neglected if the trapped particles exhibit nonlinear optical effects. Moreover, the experimental observations have revealed that the nonlinear optical effects could enhance the optical force [8,16] or modify the optical trapping potential [13].

To quantitatively appraise the trapping ability, the optical force exerted on a spherical nanoparticle arising from the linear polarization has been calculated by various approaches, such as Rayleigh scattering formulae [1], Maxwell's stress tensor [17], and discrete dipole approximation [18]. For a nonlinear optical Rayleigh particle, however, the optical force unambiguously originates from the contribution of both the linear- and nonlinear-induced polarizations. To the best of our knowledge, there is no theoretical report on the optical force exerted on a nonlinear optical Rayleigh particle beyond the linear optical regime. Alternatively, researchers directly modified the Rayleigh scattering formulae by replacing the refractive index n_0^p with $n_0^p + n_2 I$ [19–21], where I is the optical intensity, and n_0^p and n_2 are the linear and third-order nonlinear refractive indexes of particle, respectively. This phenomenological theory could interpret the self-focusing effect that increases the trapping force strength and improves the confinement of Rayleigh particles [19–21].

In this work, for the first time to our knowledge, we develop time-averaged optical forces on a nonlinear optical Rayleigh particle using high-repetition-rate femtosecond laser pulses, based on the linear and nonlinear polarization effects.

2. THEORY

For time-harmonic electromagnetic waves with a Gaussian temporal envelope, we have

$$\vec{E}(\vec{r},t)=\vec{E}_0(\vec{r})\exp(-i\omega t)\exp[-2(\ln 2)t^2/\tau_F^2], \tag{1}$$

$$\vec{B}(\vec{r},t)=\frac{1}{i\omega}\nabla\times\vec{E}(\vec{r},t), \tag{2}$$

where $\vec{E}_0(\vec{r})$ is the complex function of position in space, ω is the circular frequency, and τ_F is the full width at half-maximum (FWHM) for a Gaussian pulse. For the sake of simplicity, we only consider the pulse duration of laser pulses having $\tau_F\sim 100$ fs. Accordingly, the spectral bandwidth of the laser pulses is so narrow that the pulsed beam can be regarded as a monochromatic field. Hence the spatial and temporal characteristics of laser pulses can be treated independently.

Now we consider a spherical dielectric particle immersed in liquid (e.g., water) exhibiting a linear susceptibility χ_1 and a third-order nonlinear optical susceptibility χ_3. Besides, we assume that the particle is isotropic and the optical nonlinearity instantaneously responds to laser pulses. According to the Claussius–Mossotti equation and taking into account the radiation reaction correction [22,23], we obtain the particle-induced dipole moment originating from the linear and nonlinear polarizations as

$$\vec{p}(\vec{r},t)=\frac{\alpha_e(\vec{r},t)}{1-i\alpha_e(\vec{r},t)k^3/(6\pi\varepsilon_0)}\vec{E}(\vec{r},t), \tag{3}$$

$$\alpha_e(\vec{r},t)=4\pi\varepsilon_0 a^3\frac{(\chi_1+\chi_3|\vec{E}(\vec{r},t)|^2)}{\chi_1+\chi_3|\vec{E}(\vec{r},t)|^2+3}, \tag{4}$$

where a is the radius of the particle, $k=2\pi/\lambda$ is the wavenumber, λ is the wavelength, and ε_0 is the permittivity of free space.

Under the excitation of femtosecond laser pulses, the instantaneous optical force exerted on the Rayleigh particle ($a\ll\lambda$) for time-averaging over one pulse period T yields [24]

$$\langle\vec{F}\rangle=\frac{1}{4T}\int_{-T/2}^{T/2}\left[(\vec{p}+\vec{p}^{\,*})\cdot\nabla(\vec{E}+\vec{E}^{\,*})+\left(\frac{\partial\vec{p}}{\partial t}+\frac{\partial\vec{p}^{\,*}}{\partial t}\right)\times(\vec{B}+\vec{B}^{\,*})\right]dt, \tag{5}$$

where $*$ denotes the complex conjugate.

The stable optical trapping of nanoparticles with high-repetition-rate femtosecond laser pulses has been experimentally demonstrated [10,12]. Each ultrafast laser pulse leads to instantaneous trapping of a nanoparticle. The high-repetition-rate ensures repetitive trapping by successive pulses; hence the particle does not diffuse significantly between pulses. Typically, the pulse duration τ_F and repetition-rate ν (i.e., the inverse of the pulse period T) for a commercial Ti:sapphire oscillator are ~100 fs and 76 MHz, respectively. Substituting Eqs. (1)–(4) into Eq. (5) and considering the condition of $1/(\tau_F\nu)\to\infty$, we have

$$\langle\vec{F}\rangle=\frac{\pi\varepsilon_0 a^3\tau_F\nu}{\sqrt{\ln 2}}\mathrm{Re}[\beta(\vec{E}_0\cdot\nabla\vec{E}_0^{\,*}+\vec{E}_0\times\nabla\times\vec{E}_0^{\,*})], \tag{6}$$

with

$$\beta=\int_{-\infty}^{\infty}\frac{(\chi_1+\chi_3|\vec{E}_0|^2e^{-\zeta^2})e^{-\zeta^2}}{3+(1-2ik^3a^3/3)(\chi_1+\chi_3|\vec{E}_0|^2e^{-\zeta^2})}d\zeta. \tag{7}$$

Here, $\chi_1=\varepsilon_2^0/\varepsilon_1^0-1$, where ε_2^0 and ε_1^0 are the permittivities of the particle and the surrounding medium, respectively.

After integrating Eq. (7), we obtain the time-averaged optical forces on a nonlinear optical Rayleigh particle as

$$\langle\vec{F}\rangle=\frac{1}{4}\mathrm{Re}(\alpha)\nabla|\vec{E}_0|^2+\frac{k}{\varepsilon_0 c}\mathrm{Im}(\alpha)\langle\vec{S}\rangle_{\mathrm{Orb}}, \tag{8}$$

where

$$\langle\vec{S}\rangle_{\mathrm{Orb}}=\langle\vec{S}\rangle+\frac{\varepsilon_0 c}{2k}\mathrm{Im}[(\vec{E}_0^{\,*}\cdot\nabla)\vec{E}_0], \tag{9}$$

$$\langle\vec{S}\rangle=\frac{1}{2\mu_0\omega}\mathrm{Im}[\vec{E}_0\times(\nabla\times\vec{E}_0^{\,*})], \tag{10}$$

$$\alpha=\frac{\sqrt{\pi}\tau_F\nu}{2\sqrt{\ln 2}}(\gamma_L+\gamma_{NL}), \tag{11}$$

$$\gamma_L=\frac{\alpha_0}{1-i\alpha_0k^3/(6\pi\varepsilon_0)}, \tag{12}$$

$$\alpha_0=4\pi\varepsilon_0a^3\frac{\varepsilon_2^0/\varepsilon_1^0-1}{\varepsilon_2^0/\varepsilon_1^0+2}, \tag{13}$$

$$\gamma_{NL}=\frac{12\pi\varepsilon_0a^3}{\eta}\sum_{m=2}^{\infty}\frac{(-1)^m}{m^{1/2}}\frac{(\chi_3\eta|\vec{E}_0|^2)^{m-1}}{[3+\eta(\varepsilon_2^0/\varepsilon_1^0-1)]^m}, \tag{14}$$

$$\eta=1-2ik^3a^3/3. \tag{15}$$

Here, c and μ_0 are the speed and permeability of light in vacuum, respectively.

As described by Eq. (8), optical forces on a nonlinear nanoparticle with femtosecond laser pulses are divided into two parts: the gradient force, which is proportional to the gradient of intensity and drives the particle toward the equilibrium point, and the radiation force, which is proportional to the orbital part of the Poynting vector of the field and destabilizes the trap by pushing the particle away from the focal point. Note that Eq. (8) degenerates into the one reported previously [7,17] for a Rayleigh particle without optical nonlinearity (i.e., $\chi_3=0$). Moreover, it is demonstrated, both experimentally [10] and theoretically [25,26], that optical forces due to pulsed beam and CW beam of the same average power should be identical if the nonlinear optical effect can be neglected. Different from the conventionally optical forces arising from the interaction of optical fields with the linear polarization, the optical trapping of nonlinear optical particles originates from the linear and nonlinear polarizations. Furthermore, the optical forces exerted on the nonlinear particle strongly depend on the nonlinear susceptibility of particle and the distribution of electric field besides the other parameters related to the laser characteristics and the particle itself.

3. RESULTS AND DISCUSSION

To trap and manipulate nanoparticles in optical tweezers, generally, an x-polarized Gaussian beam is tightly focused by a high numerical-aperture (NA) objective lens. Theoretically, the electric field distribution $\vec{E}_0(\vec{r})$ in the focal region of an aplanatic lens can be expressed as [27]

$$\vec{E}_0(\vec{r}) = \frac{E_{00}\mathrm{i}}{\lambda}\begin{Bmatrix}[I_0 + \cos(2\varphi)I_2]\vec{e}_x \\ \sin(2\varphi)I_2\vec{e}_y \\ 2\mathrm{i}\cos\varphi I_1\vec{e}_z\end{Bmatrix} \tag{16}$$

with

$$I_0 = \int_0^{\vartheta} l(\theta)\mathrm{e}^{\mathrm{i}kz\cos\theta}(1+\cos\theta)J_0(kr\sin\theta)\mathrm{d}\theta, \tag{17}$$

$$I_1 = \int_0^{\vartheta} l(\theta)\sin\theta\mathrm{e}^{\mathrm{i}kz\cos\theta}J_1(kr\sin\theta)\mathrm{d}\theta, \tag{18}$$

$$I_2 = \int_0^{\vartheta} l(\theta)\mathrm{e}^{\mathrm{i}kz\cos\theta}(1-\cos\theta)J_2(kr\sin\theta)\mathrm{d}\theta. \tag{19}$$

Here, $l(\theta) = \exp(-\sin^2\theta/\sin^2\vartheta)\sin\theta(\cos\theta)^{1/2}$. r, φ, and z are the polar radius, azimuthal angle, and axial position in the cylindrical coordinate system for the observational point, respectively. $J_m(\cdot)$ is the mth-order Bessel function of the first kind. $\vartheta = \arcsin(\mathrm{NA}/n_0^w)$ is the maximal angle determined by the NA of the objective lens in the image space, where $n_0^w = (\varepsilon_1^0)^{1/2}$ is the linear refractive index in the image space. According to the law of conservation of energy, the coefficient E_{00} is given by $|E_{00}|^2 = 4n_0^w P_{\mathrm{peak}}/(\pi\varepsilon_0 c\mathrm{NA}^2)$, where $P_{\mathrm{peak}} = 2(\ln 2)^{1/2}P/(\pi^{1/2}\tau_F\nu)$ and P is the average power of laser pulses.

Substituting Eq. (16) into Eq. (8), one could calculate the time-averaged optical forces on an optical nonlinear Rayleigh particle by tightly focused linearly polarized Gaussian beam. It should be noted that the value of $\varepsilon_0 c\mathrm{Im}[(\vec{E}_0^* \cdot \nabla)\vec{E}_0]/(2k)$ in Eq. (9) is proportional to the nonuniform distribution of the spin density of the light field [17]. When the input beam is a linearly polarized beam, however, this value becomes negligible and can be ignored. Hence, the radiation force expressed by Eq. (8) is only proportional to the Poynting vector $\langle\vec{S}\rangle$ in the following analysis.

In addition to the characteristics of the light field, the polarization induced by the external optical field in the particle undoubtedly plays a crucial role in the magnitude and distribution of the optical force. As described by Eq. (14), the nonlinear polarization is related to both the third-order nonlinear optical susceptibility χ_3 and the distribution of electric field. For the sake of simplicity, we only consider the Rayleigh dielectric particle exhibiting the Kerr nonlinearity. In this case, the third-order nonlinear optical susceptibility χ_3 is related to the third-order nonlinear refractive index n_2 through the conversion formula $\mathrm{Re}[\chi_3] = n_2\varepsilon_2^0\varepsilon_0 c/(3\varepsilon_1^0)$. In general, the nonlinear refractive index of particles ranges in magnitude from 10^{-14} to 10^{-20} m^2/W. Note that the moderate magnitude of n_2 is taken in this work [21]. Without loss of generality, the particle is assumed to be immersed in water. Consequently, the linear refractive indexes of water and particle are taken to be $n_0^w = (\varepsilon_1^0)^{1/2} = 1.33$ and $n_0^p = (\varepsilon_2^0)^{1/2} = 1.58$, respectively. For numerical calculations, the other parameters are chosen to be $\lambda = 800$ nm, $\tau_F = 100$ fs, $\nu = 76$ MHz, and the average-power of laser pulses $P = 100$ mW in the entire analysis. Using Eq. (8), we investigated both the distribution and the magnitude of the optical forces exerted on the nonlinear optical Rayleigh particle.

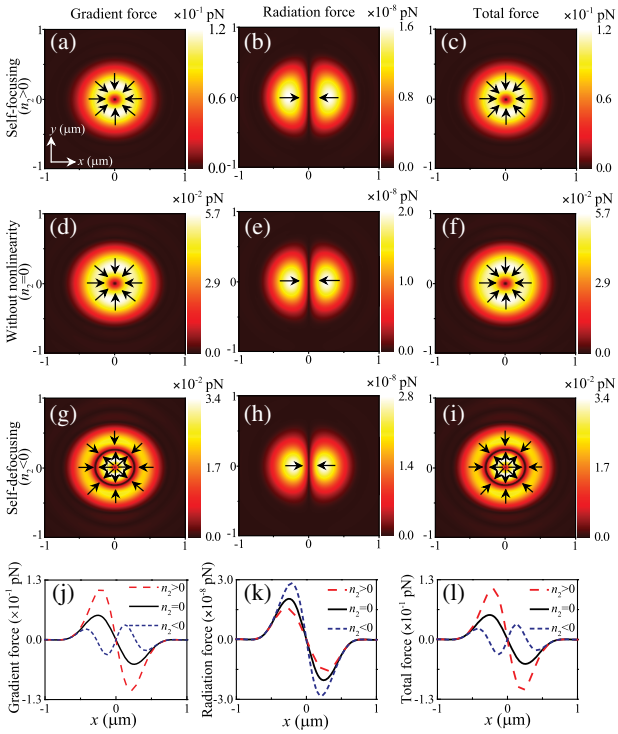

Fig. 1. Transverse force distributions produced by tightly focused laser pulses for the particle with self-focusing ($n_2 = 5.9\times10^{-17}$ m^2/W), without nonlinearity ($n_2 = 0$), and with self-defocusing ($n_2 = -5.9\times10^{-17}$ m^2/W) in the x-y plane ($z = 0$), by taking NA = 0.85 and $a = 40$ nm. The magnitudes and directions of the transverse forces are illustrated by the colorbar and arrows in (a)–(i), respectively. (j)–(l) give the force profiles along the x direction shown in the above three rows.

Figure 1 shows the distributions of the transverse forces produced by tightly focused laser pulses for the particle with self-focusing and self-defocusing effects in the x-y plane ($z = 0$), by taking three different values of n_2 (i.e., 5.9×10^{-17}, 0, -5.9×10^{-17} m^2/W), NA = 0.85, and $a = 40$ nm. Here, the transverse force is the vector superposition of the x-direction and y-direction forces, and the magnitude of the transverse force is defined as $(F_x^2 + F_y^2)^{1/2}$. For comparison, both the magnitude and the distribution of the optical force on the particle without nonlinearity ($n_2 = 0$) are also shown in the second row of Fig. 1. It is shown that the distributions of the gradient force nearly maintain the circular symmetry in the transverse plane, whereas the corresponding radiation forces exhibit a fan-shaped structure with the two-fold rotation symmetry. It is noteworthy that the magnitude of the radiation forces is negligible compared with that of the gradient forces. Consequently, the distribution of total forces can be nearly regarded to be circular.

For the particle with self-focusing effect (i.e., $n_2 > 0$), the distribution of forces displayed in the first row of Fig. 1 is almost identical to that of the particle without nonlinearity ($n_2 = 0$) shown in the second row of Fig. 1. Moreover, the total force always directs to the position of the focal point to produce a force balance. However, the magnitude of the total force exerted on the self-focusing particle is about two times larger than that on the linear particle. In the optical trapping experiments, it is expected that the transverse trapping efficiency and stiffness of the self-focusing particle are larger than those of the linear particle. Obviously, the nonlinear polarization arising from the self-focusing effect improves the particle trapping ability, which is consistent with the reported experimental observations [8,16]. Under the excitation of intense femtosecond laser pulses, the effective refractive index $n_0^p + n_2 I(r, \varphi, z)$ of the self-focusing particle ($n_2 > 0$) is larger than that of the linear particle ($n_2 = 0$). Accordingly, the self-focusing particle bends the light stronger than the same particle without nonlinearity under the same illumination condition, resulting in stronger gradient force exerted on the self-focusing particle than that on the linear particle [28].

For the self-defocusing particle (i.e., $n_2 < 0$), interestingly, both the distribution and the magnitude of the transverse force are quitely different from those of the self-focusing particles and the linear particle. As shown in Fig. 1(i), the distribution of the total force exerted on the self-defocusing particle exhibits the double-ring pattern. Furthermore, the magnitude of the total force on the self-defocusing particle is smaller than that on the linear particle ($n_2 = 0$). This special distribution of the transverse force shown in Fig. 1(i) can be interpreted for the following reasons. For the case of $n_2 < 0$, a spatial-variant Gaussian-intensity distribution in transverse can induce a negative lens effect due to the presence of space-dependent refractive-index change $n_2 I(r, \varphi, z)$. Hence, the contributions of the linear and nonlinear polarizations to the gradient force are opposite to each other. At relative weak intensity, the nonlinear polarization is not large enough, and the force exerted on the nonlinear particle is similar to that on the linear particle except for the reduced force. Under the excitation of high intensity, however, the force direction at the center and edge of the focused beam will be reversed, giving rise to the double-ring distribution of the transverse force.

Figure 2 illustrates the distributions of the longitudinal forces on the nonlinear particles produced by focused laser pulses in the x-z plane ($y = 0$), by taking three different values of n_2 (i.e., 5.9×10^{-17}, 0, -5.9×10^{-17} m^2/W), NA = 0.85, and $a = 40$ nm. Different from the transverse forces in the focal plane mainly originating from the gradient forces shown in Fig. 1, the magnitude of longitudinal gradient forces is comparable with those of the radiation forces. Owing to the self-focusing effect of the particle, the longitudinal gradient force increases and the radiation force decreases, in contrast with those on the linear particle. As a result, the self-focusing particle with femtosecond laser pulses forms a stable 3D trap in the focal region and increases the trapping efficiency and stiffness, which has been validated by the reported experiment [29]. On the contrary, for the particle exhibiting the self-defocusing effect, both the decreased longitudinal gradient force and the enhanced radiation force destabilize the trap by pushing the

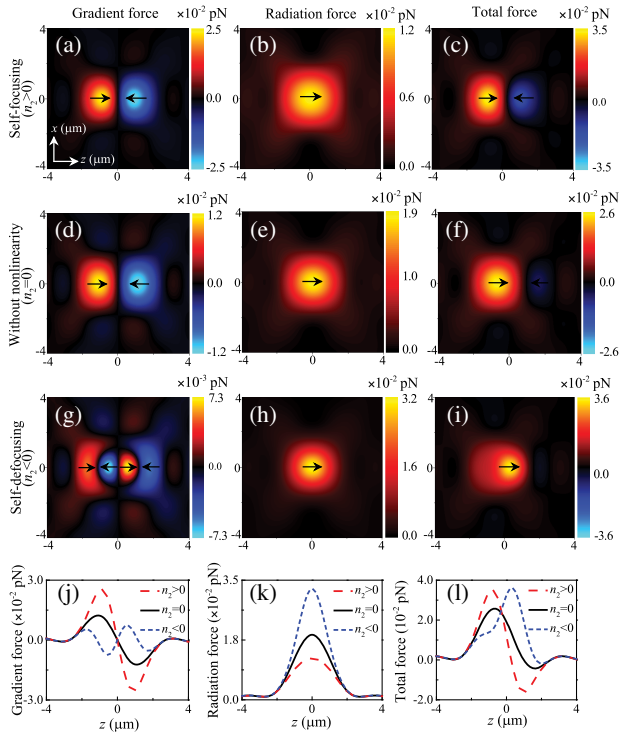

Fig. 2. Longitudinal force distributions produced by tightly focused laser pulses for the particle with self-focusing ($n_2 = 5.9 \times 10^{-17}$ m^2/W), without nonlinearity ($n_2 = 0$), and with self-defocusing ($n_2 = -5.9 \times 10^{-17}$ m^2/W) in the x-z plane ($y = 0$), by taking NA = 0.85 and $a = 40$ nm. The bottom row gives the force profiles along the z direction shown in the above three rows. Arrows in the figures denote the directions of the longitudinal forces.

particle away from the focal plane. That is, at relatively low power of the laser pulses, the self-defocusing particle is trapped at the focal plane because of the weak optical nonlinearity. With increasing the power under the pulsed excitation, interestingly, the trapped particle will be ejected axially along the direction of the beam's propagation owing to the strong longitudinal force arising from the self-defocusing effect. This theoretical result successfully explains the puzzling experimental phenomena that the optical trapping is destabilized with increasing power under pulsed excitation only [12,15].

Except for the sign of optical nonlinearity, the optical forces exerted on nonlinear optical Rayleigh particles strongly depend on the magnitude of nonlinear refractive index n_2, the numerical aperture of an objective lens NA, and the size of the nanoparticle a. Figure 3 shows the force profiles along the x direction for $y = 0$ and $z = 0$ when one parameter changes. Here, the parameters used for numerical simulations, if they are not the changing one, are $n_2 = 6 \times 10^{-17}$ m^2/W, NA = 0.85, and $a = 40$ nm. As shown in the first column of Fig. 3, the positive (or negative) optical forces mean that their direction is along the $+x$ (or $-x$) direction. Clearly, the self-focusing particle can be easily trapped along the x direction at the focal plane due to the existence of the equilibrium point. Furthermore, the magnitude of optical forces increases when the value of n_2, NA, or a increases. As is well known, the larger the magnitude of optical force is, the higher the

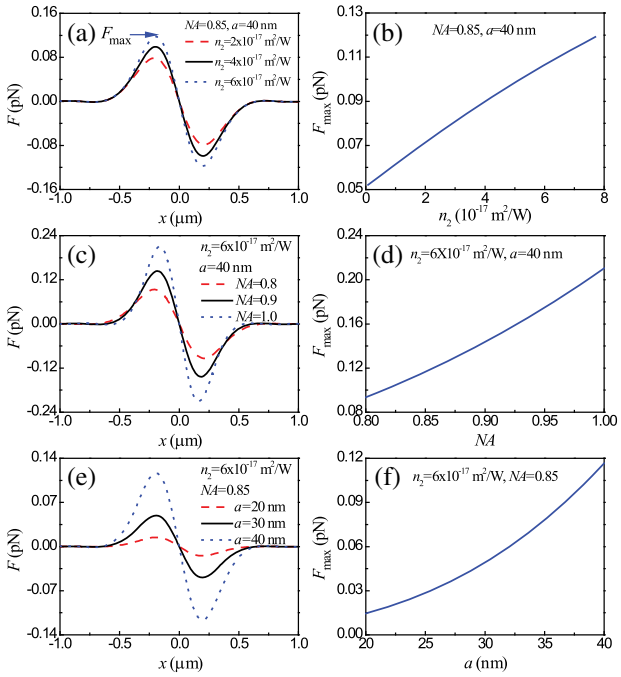

Fig. 3. Force profiles along the x direction for $y = 0$ and $z = 0$. (a) Different values of n_2, NA = 0.85, and $a = 40$ nm. (c) Different values of NA, $n_2 = 6 \times 10^{-17}$ m^2/W, and $a = 40$ nm. (e) Different values of a, $n_2 = 6 \times 10^{-17}$ m^2/W, and NA = 0.85. (b), (d), and (f) are the maximum force F_{max} versus n_2, NA, and a, respectively.

optical trapping efficiency and stiffness are. As shown in the second column of Fig. 3, it is found that the maximum values of the optical forces, F_{max}, are monotonously nonlinear increasing functions of n_2, NA, or a. In order to increase the optical trapping efficiency and stiffness in optical tweezers, one should trap the large-sized particles with large optical nonlinearity using high NA objective lens.

To form a stable particle trap, the potential generated by the gradient force must be deep enough to overcome the kinetic energy of the particle in Brownian motion, $k_B T$, where k_B is Boltzmann constant, and T is the absolute temperature of the ambience. In the optical trapping, the heating effect unavoidably exists and increases the temperature of the trapped particles and surrounding medium, especially for absorbing particles. In this work, we restrict our attention to nonabsorbing particles with refractive nonlinearity. Hence, the heating effect is limited, and the temperature raised by the optical trapping is negligible. An assumption that the room temperature of $T = 300$ K is used to calculate the potential depth is reasonable. The potential depth can be estimated by $U = -\int \vec{F} \cdot d\vec{r}$, which is the work done by the optical force along the trapping length direction [30]. Figure 4 shows the trapping potential along the x and z directions for the particles with three different values of n_2 (i.e., 5.9×10^{-17}, 0, -5.9×10^{-17} m^2/W), by taking NA = 0.85 and $a = 40$ nm. As shown in Fig. 4(a), the potential depths for three types of particles are larger than 1 $k_B T$. Accordingly, the particles with and without nonlinearity can be captured along the x direction. The potential of the self-focusing particle becomes deeper than that of the linear

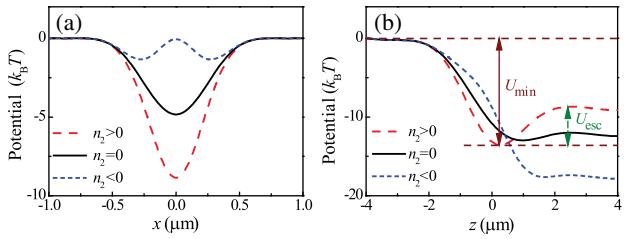

Fig. 4. Trapping potential along (a) x direction and (b) z direction with three different values of n_2 (i.e., 5.9×10^{-17}, 0, -5.9×10^{-17} m^2/W), NA = 0.85, and $a = 40$ nm.

particle, indicating that the self-focusing effect enhances the trapping ability. Surprisingly, for the particle exhibiting the self-defocusing nonlinearity, the potential splits into two off-axis trapping sites along the x direction, which is supported by the reported experiments [13]. For the trapping potential along the z direction shown in Fig. 4(b), there are two important parameters: one is the absolute depth of the potential minimum U_{min}, and the other is the potential barrier U_{esc} that directly relates to the trapping efficiency. As shown in Fig. 4(b), the self-focusing effect increases the values of U_{min} and U_{esc} and then improves the confinement of particles. However, the potential barrier U_{esc} of the self-defocusing particle is less than 1 $k_B T$, resulting in the destabilization of the particle in the axial direction.

4. CONCLUSIONS

In summary, for the first time to our knowledge, we have developed time-averaged optical forces exerted on a nonlinear optical Rayleigh particle using high-repetition-rate femtosecond laser pulses, based on linear and nonlinear polarizations. We have investigated the characteristics of the transverse and longitudinal optical forces for particles exhibiting self-focusing and self-defocusing effects. It is shown that the self-focusing effect increases the trapping force strength and improves the confinement of particles, whereas the self-defocusing effect leads to the splitting of the potential well at the focal plane and destabilizes the optical trap, resulting in ejections of trapped particles along the direction of the beam's propagation. Experimentally, the optical forces exerted on the nonlinear optical particles are directly related to the trapping stiffness. It is expected that the self-focusing (or self-defocusing) effect increases (or decreases) the trapping efficiency and stiffness. Our results successfully explain the reported experimental observations and provide theoretical support for capturing nonlinear nanoparticles with femtosecond laser trapping.

Funding. National Natural Science Foundation of China (NSFC) (11474052, 11504049, 11774055, 61535003); Natural Science Foundation of Jiangsu Province, China (BK20171364); National Key Basic Research Program of China (2015CB352002).

REFERENCES

1. A. Ashkin, J. M. Dziedic, J. E. Bjorkholm, and S. Chu, "Observation of a single-beam gradient force optical trap for dielectric particles," Opt. Lett. **11**, 288–290 (1986).

2. J. R. Moffitt, Y. R. Chemla, S. B. Smith, and C. Bustamante, "Recent advances in optical tweezers," Annu. Rev. Biochem. **77**, 205–228 (2008).
3. I. Heller, T. P. Hoekstra, G. A. King, E. J. G. Peterman, and G. J. L. Wuite, "Optical tweezers analysis of DNA-protein complexes," Chem. Rev. **114**, 3087–3119 (2014).
4. L. Huang, H. Guo, J. Li, L. Ling, B. Feng, and Z. Y. Li, "Optical trapping of gold nanoparticles by cylindrical vector beam," Opt. Lett. **37**, 1694–1696 (2012).
5. E. Vetsch, D. Reitz, G. Sague, R. Schmidt, S. T. Dawkins, and A. Rauschenbeutel, "Optical interface created by laser-cooled atoms trapped in the evanescent field surrounding an optical nanofiber," Phys. Rev. Lett. **104**, 203603 (2010).
6. C. Min, Z. Shen, J. Shen, Y. Zhang, H. Fang, G. Yuan, L. Du, S. Zhu, T. Lei, and X. Yuan, "Focused plasmonic trapping of metallic particles," Nat. Commun. **4**, 2891 (2013).
7. A. Canaguier-Durand, A. Cuche, C. Genet, and T. W. Ebbesen, "Force and torque on an electric dipole by spinning light fields," Phys. Rev. A **88**, 033831 (2013).
8. W. Chiang, T. Okuhata, A. Usman, N. Tamai, and H. Masuhara, "Efficient optical trapping of CdTe quantum dots by femtosecond laser pulses," J. Phys. Chem. B **118**, 14010–14016 (2014).
9. I. S. Park, S. H. Park, S. W. Lee, D. S. Yoon, and B. Kim, "Quantitative characterization for dielectrophoretic behavior of biological cells using optical tweezers," Appl. Phys. Lett. **104**, 053701 (2014).
10. B. Agate, C. Brown, W. Sibbett, and K. Dholakia, "Femtosecond optical tweezers for *in-situ* control of two-photon fluorescence," Opt. Express **12**, 3011–3017 (2004).
11. L. Wang and C. Zhao, "Dynamic radiation force of a pulsed Gaussian beam acting on Rayleigh dielectric sphere," Opt. Express **15**, 10615–10621 (2007).
12. J. C. Shane, M. Mazilu, W. M. Lee, and K. Dholakia, "Effect of pulse temporal shape on optical trapping and impulse transfer using ultrashort pulsed lasers," Opt. Express **18**, 7554–7568 (2010).
13. Y. Jiang, T. Narushima, and H. Okamoto, "Nonlinear optical effects in trapping nanoparticles with femtosecond pulses," Nat. Phys. **6**, 1005–1009 (2010).
14. W. Y. Chiang, A. Usman, and H. Masuhara, "Femtosecond pulse-width dependent trapping and directional ejection dynamics of dielectric nanoparticles," J. Phys. Chem. C **117**, 19182–19188 (2013).
15. T. H. Liu, W. Y. Chiang, A. Usman, and H. Masuhara, "Optical trapping dynamics of a single polystyrene sphere: continuous wave versus femtosecond lasers," J. Phys. Chem. C **120**, 2392–2399 (2016).
16. M. Gu, H. Bao, X. Gan, N. Stokes, and J. Wu, "Tweezing and manipulating micro- and nanoparticles by optical nonlinear endoscopy," Light: Sci. Appl. **3**, e126 (2014).
17. S. Albaladejo, M. I. Marqués, M. Laroche, and J. J. Saenz, "Scattering forces from the curl of the spin angular momentum of a light field," Phys. Rev. Lett. **102**, 113602 (2009).
18. S. Simpson and S. Hanna, "Application of the discrete dipole approximation to optical trapping calculations of inhomogeneous and anisotropic particles," Opt. Express **19**, 16526–16541 (2011).
19. R. Pobre and C. Saloma, "Radiation force exerted on nanometer size non-resonant Kerr particle by a tightly focused Gaussian beam," Opt. Commun. **267**, 295–304 (2006).
20. L. Jauffred and L. B. Oddershede, "Two-photon quantum dot excitation during optical trapping," Nano Lett. **10**, 1927–1930 (2010).
21. A. Devi and K. De, "Theoretical investigation on nonlinear optical effects in laser trapping of dielectric nanoparticles with ultrafast pulsed excitation," Opt. Express **24**, 21485–21496 (2016).
22. B. T. Draine, "The discrete-dipole approximation and its application to interstellar graphite grains," Astrophys. J. **333**, 848–872 (1988).
23. M. Nieto-Vesperinas, J. J. Sáenz, R. Gómez-Medina, and L. Chantada, "Optical forces on small magnetodielectric particles," Opt. Express **18**, 11428–11443 (2010).
24. P. Chaumet and M. Nieto-Vesperinas, "Time-averaged total force on a dipolar sphere in an electromagnetic field," Opt. Lett. **25**, 1065–1067 (2000).
25. J. L. Deng, Q. Wei, and Y. Z. Wang, "Numerical modeling of optical levitation and trapping of the "stuck" particles with a pulsed optical tweezers," Opt. Express **13**, 3673–3680 (2005).
26. N. Preez-Wilkinson, A. B. Stilgoe, T. Alzaidi, H. Rubinsztein-Dunlop, and T. A. Nieminen, "Forces due to pulsed beams in optical tweezers: linear effects," Opt. Express **23**, 7190–7208 (2015).
27. M. Gu, *Advanced Optical Imaging Theory* (Springer, 2000), Chap. 6.
28. A. Devi and A. K. De, "Theoretical investigation on optical Kerr effect in femtosecond laser trapping of dielectric microspheres," J. Opt. **19**, 065504 (2017).
29. A. K. De, D. Roy, A. Dutta, and D. Goswami, "Stable optical trapping of latex nanoparticles with ultrashort pulsed illumination," Appl. Opt. **48**, G33–G37 (2009).
30. G. Rui and Q. Zhan, "Trapping of resonant metallic nanoparticles with engineered vectorial optical field," Nanophotonics **3**, 351–361 (2014).